Arch. Metall. Mater., Vol. 61 (2016), No 2B, p. 1109–1114

DOI: 10.1515/amm-2016-0186

A. ZIEWIEC*#

STUDY OF THE WELDABILITY OF AUSTENITIC PH STEEL FOR POWER PLANTS

The article presents the results of Transvarestraint test of a modern precipitation hardened steel X10CrNiCuNb18-9-3 with copper. For comparison, the results of tests of conventional steel without the addition of copper X5CrNi18-10 are presented. The total length of all cracks and the maximum length of cracks were measured. The study of microstructure (LM, SEM) showed that the austenitic stainless steel X10CrNiCuNb18-9-3 is very prone to hot cracking. After performing the Transvarestraint tests three types of cracks were observed: solidification cracks occurring during crystallization, liquation cracks due to segregation in the heat affected zone (HAZ) and surface cracks. Niobium carbonitrides dispersed in the bands of segregation are the reason of high susceptibility to liquation cracking. Segregation of copper occurring during solidification causes of surface cracking. A combined effect of copper and stresses contributes to formation of hot microcracks. These microcracks propagate to a depth of 20-30 μm.

Keywords: power plants, Super 304H, DMV 304HCu steel, X10CrNiCuNb18-9-3 steel, austenitic PH stainless steels, hot cracking

1. Introduction

For many years there has been a tendency to increase the temperature and pressure in a newly launched units of power plants. The purpose of incerase has been to improve the efficiency and reducing emission of CO_2 into the atmosphere. Therefore the material should withstand the loads operating for a long time at temperatures above 600°C and pressure at the level at least 28.5 MPa [1]. The conventional austenitic steel X5CrNi18-10 do not meet these requirements due to too low creep resistance. This resulted in the necessity of replacing the steel with other austenitic stainless steels and nickel alloys [2]. One of the newest austenitic steels currently used in the power industry, designed to operate at high temperatures is X10CrNiCuNb18-9-3 steel (commercial name of the steel: a Super 304H, DMV 304HCu). The X10CrNiCuNb18-9-3 steel appears to be very promising, mainly due to the high resistance to oxidation, corrosion, creep, and relatively low cost of production [3,4]. It is one of the most common heat-resistant 18Cr-9Ni type steel with the addition of Cu and Nb.

In as-received state the X10CrNiCuNb18-9-3 steel is characterized by austenitic structure of precipitates of Nb(C,N) niobium carbonitrides, and fine dispersive precipitates that are enriched in copper, and are located mainly inside the grains of austenite [1]. It has very good properties at high temperatures and particularly high creep resistance at 650°C. The addition of 3% Cu to the steel aimed at increasing the corrosion resistance resulted in elevated temperature strength and the creep strengh in the temperature range 650-750°C [3]. X10CrNiCuNb18-9-3 steel is used for the construction of tubes, and thin parts of boilers. It is well known that these parts of boilers should withstand not only high temperature of approx. 600°C, but also a substantial pressure for a sufficiently long period of service. The construction of such devices is complicated, and in spite of limiting the amount of possible joints, it is necessary to connect the individual pipe sections by welding. The quality has to be perfect, because every crack can cause failure [5-6]. It is believed [7] that the X10CrNiCuNb18-9-3 steel is well weldable. The preheating is not necessary before welding, because this steel is not susceptible to hydrogen cracking. Post-weld heat treatment is applied only for improving the corrosion resistance. However, attention should be paid to some problems with the weldability of the steels. The X10CrNiCuNb18-9-3 steel weld is austenitic, therefore it can be susceptible to hot cracking.

Some research has been conducted on the evaluation of the steel microstructure, mechanical properties [1,5] and creep resistance [4,8]. There is no reference concerning the weldability of the steel. Therefore, this work is devoted to evaluation of the weldability using the Transvarestraint test.

2. Experimental

The study was carried out on two austenitic stainless steels: modern X10CrNiCuNb18-9-3 precipitation hardened steel with copper and the other grade for reference was the conventional X5CrNi18-10 steel without the addition of copper. The chemical composition of the studied steels is given in Table 1.

* AGH UNIVERSITY OF SCIENCE AND TECHNOLOGY

Corresponding author: aziewiec@edu.agh.pl

TABLE 1

Chemical composition of studied steels

Steel grade	Concentration, wt %											
	C	Si max	Mn max	P max	S max	Cr	Ni	Nb	Cu	N	Al.	B
X10CrNiCuNb18-9-3	0,07	0,30	1,00	0,04	0,01	17,0-19,0	7,5-10,5	0,30-0,60	2,50-3,50	0,05-0,12	0,003-0,03	0,001-0,01
X5CrNi18-10	0,07	1,00	2,00	0,045	0,015	17,5-19,5	8,0-10,5	–	–	0,011 max	–	–

The samples were subjected to Transvarestraint test. This test allows determination of the effect of deformation on the susceptibility to hot cracking of the base material and the weld. Changing the radius of the die blocks enables change of the deformation value. Deformation induced by test caused the appearance of cracks in the weld or HAZ of the base material. In order to assess the technological strength of the material the following features should be determined: minimal deformation causing cracks, so-called cracking threshold, i.e. the total length of all cracks, the maximum crack length. Diagram presenting the Transvarestraint test is shown in Fig. 1.

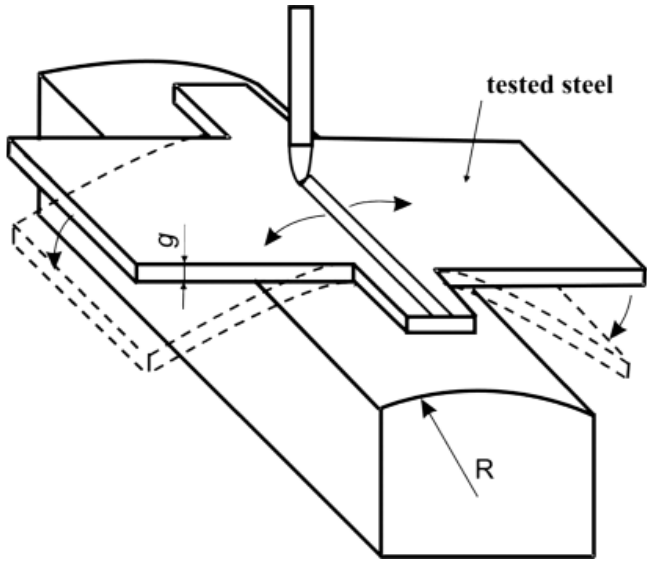

Fig. 1. Diagram presenting the Transvarestraint test [9]

The study was carried out on a universal testing system build in the Department of Physical Metallurgy & Powder Metallurgy of the AGH University of Science and Technology. The testing system enable performing both Varestraint and Transvarestraint tests. The test was based on the welding of the sample using GTAW method. After switching off the arc, the pneumatically controlled die block was moved up. This led to bending of the sample mounted in a shackle that resulted in matching the sample curvature to the shape of the removable die block upper surface. During the Transvarestraint test the subsequent deformation was performed on the die blocks having the decreasing curvature radius of the upper surface (R = 135, 110, 85, 38, 30 and 17 mm). The dimensions of the samples were 220×50×5 mm for X10CrNiCuNb18-9-3 steel and 220×50×4 mm for X5CrNi18-10 steel. In order to average the results of the measurements the two test series were performed. Moreover, in order to check, whether the welding without deformation causes cracking of the weld, the samples were autogenous welded without deformation.

The parameters of welding by GTAW method are the following: DC current of 80A, 2 mm diameter tungsten electrode, argon as shielding gas, the flow of shielding gas: 10 l/min. The surfaces of samples (plates) were ground using abrasive paper in order to remove the surface layer of oxides and contaminants. Then total crack length and maximum crack for the subsequent values of curvature radius of the upper plane of the die block were measured

Measurements were performed on a stereoscopic microscope at magnification of 10×. The deformation was calculated using the relationship [9]: $\varepsilon = g/2R$, where ε – deformation, g – sample thickness, mm, R – curvature radius of the upper face of the die block, mm. Microscopic examination was performed on a light microscope Leica DM LM and the scanning microscope: JEOL JEM-6610 with energy dispersive spectrometer (EDS) and Stereoscan 120. The microsections were made parallel to welded surface and perpendicular to the weld. Then the sections were electrolytically etched in 10% aqueous solution of CrO_3.

3. Results

Table 2 summarizes the results of the measurements the total length of all cracks and the maximum length of the cracks, while Figures 2 and 3 show a graphical dependence of total crack length and maximum crack length on the size of the applied deformation. It is apparent from data presented in Table 2 and in Fig. 2 and 3 that even a deformation lower than 2% results in cracks in the weld of X10CrNiCuNb18-9-3 steel. However, in case of the X5CrNi18-10 steel even deformation higher than 11% does not cause cracking. This indicates that the X10CrNiCuNb18-9-3 steel is more susceptible to hot cracking compared to the steel X5CrNi18-10 steel. When the samples were only autogenously welded, without the application of the deformation, there were no cracks present in both samples.

Figure 4a-c shows examples of the surface appearance of the X10CrNiCuNb18-9-3 steel weld after the various variants of deformation. For comparison Fig. 4d shows the appearance of X5CrNi18-10 steel weld without cracks.

Intergranular apprearance of the fracture (Fig. 5) with large plane regions confirms that these cracks are due to solidi-

TABLE 2

The results of Transvarestraint test

Steel grade	No.of sample	The radius of curvature of the die block φ [mm]	The steel thickness [mm]	Deformation ε [%]	The total length of cracks [mm]	The maximum length of the crack [mm]
X10CrNiCuNb18-9-3	0C	–	5	0	Not found	Not found
	1C	135	5	1,85	2,72	0,95
	2C	110	5	2,27	3,22	0,98
	3C	85	5	2,94	3,54	1,04
	4C	38	5	6,58	3,84	1,02
	5C	30	5	8,33	4,45	1,22
	6C	17	5	14,71	4,82	1,46
X5CrNi18-10	0	–	4	0	Not found	Not found
	1	135	4	1,48	Not found	Not found
	5	30	4	6,67	Not found	Not found
	6	17	4	11,76	Not found	Not found

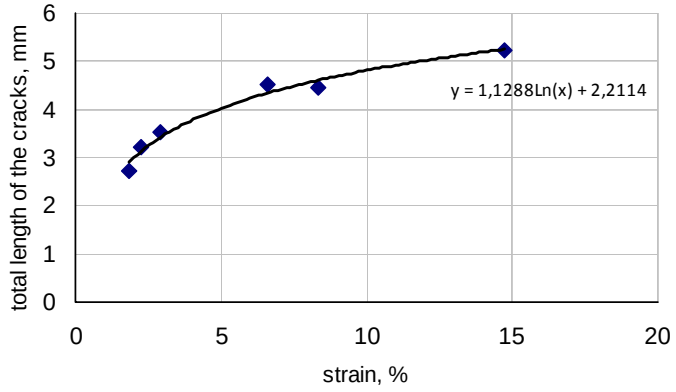

Fig. 2. Dependence of the total length of the cracks on the strain of samples

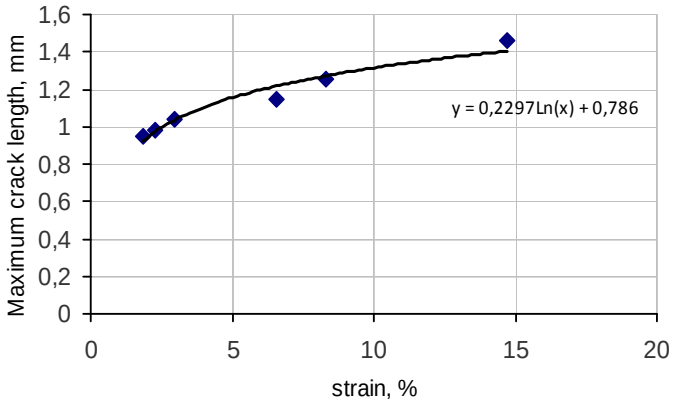

Fig. 3. The dependence of the maximum crack length on the strain of samples

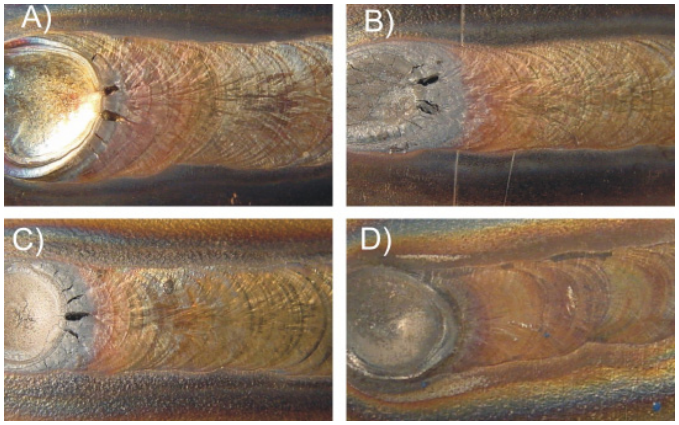

Fig. 4. The surface appearance of the samples after the Transvarestraint test; a) X10CrNiCuNb18-9-3 steel with visible cracks (ε = 1.85%), b) X10CrNiCuNb18-9-3 steel (ε = 8.33%), c) X10CrNiCuNb18-9-3 steel (ε = 14.71%), d) X5CrNi18-10 steel, no cracks (ε = 11.7%)

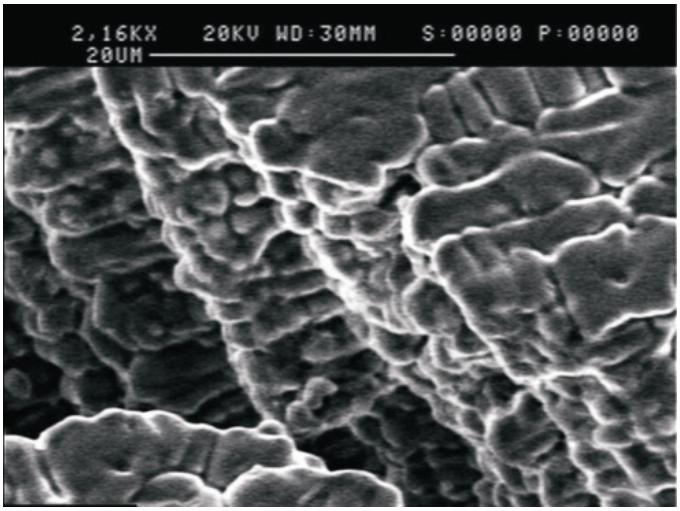

Fig. 5. SEM. Hot cracks in the weld of X10CrNiCuNb18-9-3 steel

fication cracking. Solidification cracks are formed in the area of the two-phase: liquid + austenite and a large crack length a maximum of approx. 1.5 mm indicates a wide range of solidification temperatures of the X10CrNiCuNb18-9-3 steel, and therefore the high solidification cracking susceptibility of the studied steel.

The second type of cracks in the studied steels were HAZ liquation cracks which, in the presence of tensile stresses and strains transfer to the weld (Fig. 6, 7). The liquation cracks are formed near the niobium carbides, where migrating grain boundary stopped. In the vicinity of niobium carbide the melting of the adjacent austenite occurs and a liquid enriched in niobium of a low melting temperature is formed [10]. The stresses result in spreading of the liquid on the grain boundaries. Fig. 8 shows an example of microcracks located at the grain boundaries and the eutectic carbonitrides of Nb (C, N).

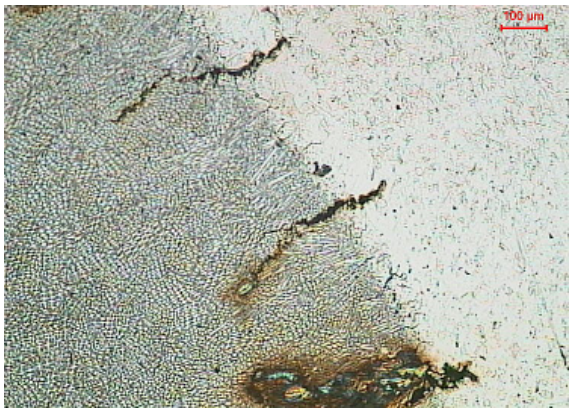

Fig. 6. LM, liquation cracks in the HAZ of X10CrNiCuNb18-9-3 steel

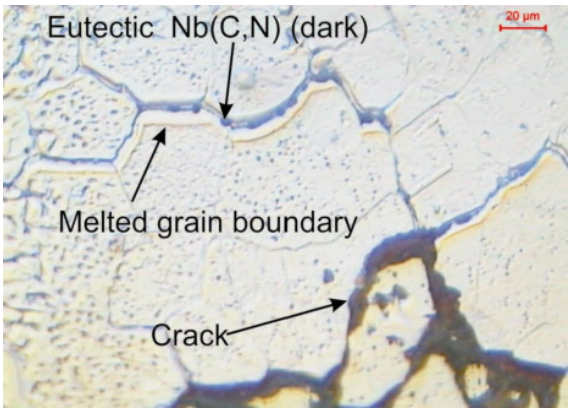

Fig. 7. LM, liquation cracks in the HAZ of X10CrNiCuNb18-9-3 steel, higher magnification

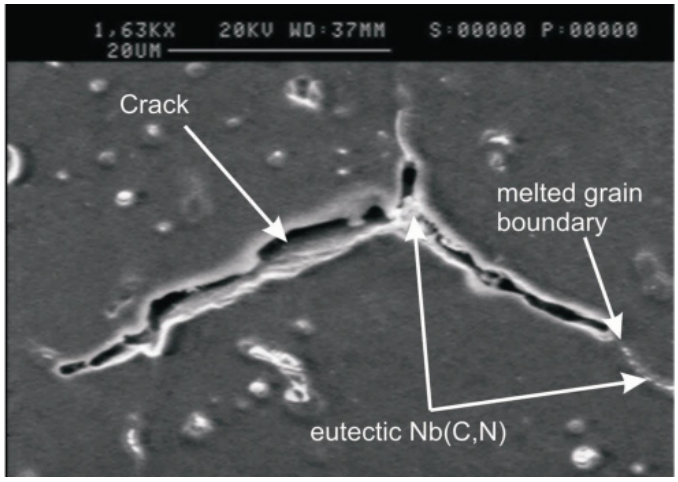

Fig. 8. SEM, Microcracks at the melted grain boundaries and the eutectic carbonitrides of Nb (C, N)

Reducing the volume of the liquid during the solidification and the strain caused by shrinkage results in formation of the liquation cracks. Inside these cracks, remaining niobium-rich liquid solidifies as eutectic shown in Figure 9a. SEM investigations showed enrichment in Nb area around the precipitates. An example of EDS analysis shown in Fig. 9b.

Appart from solidification cracks in the weld and liquation cracks in the HAZ, the investigated steel contains the surface cracks in HAZ (Fig. 10). Cracks are located uniquely at the depth of 20-30 µm. The investigations have shown that these cracks are small and the damage of the grain boundaries are decorated with oxides (Fig. 11). Table 3 presents the EDS results showing the chemical composition in the various areas of the welded joint.

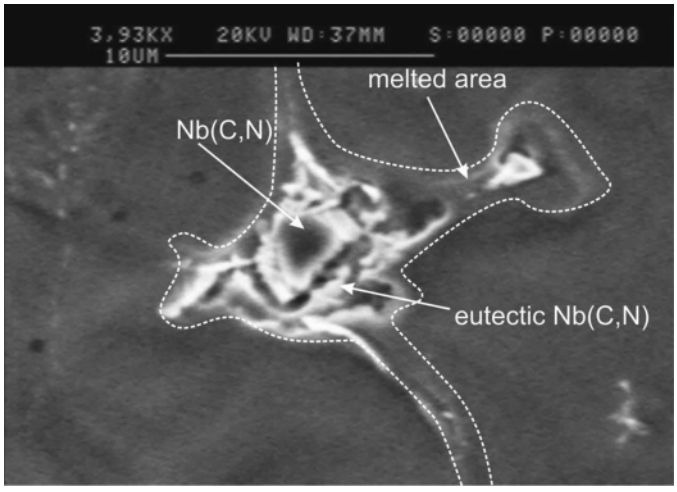

a)

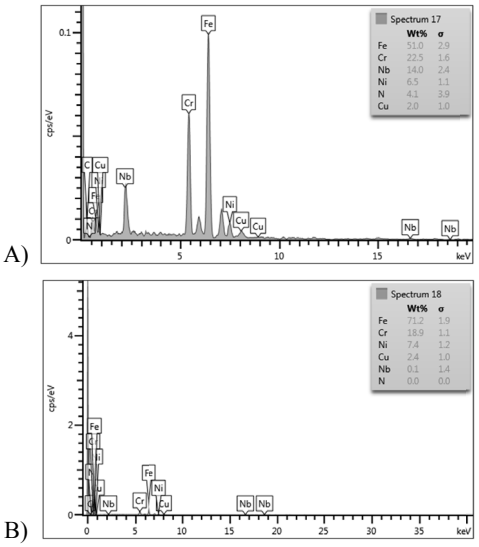

b)

Fig. 9. a) SEM micrograph; the area melted near the niobium carbonitride and subsequently resolidify in the form of eutectic, b) EDS analysis from the carbonitride (A) and the area outside the carbonitrides (B)

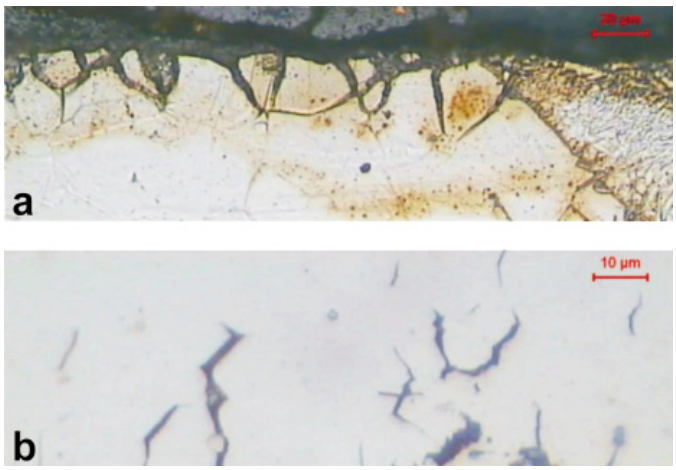

Fig. 10. LM, damage of the grain boundaries in the HAZ; a) The metallographic section perpendicular to surface of the sheet b) metallographic section (not etched) parallel to the sheet surface

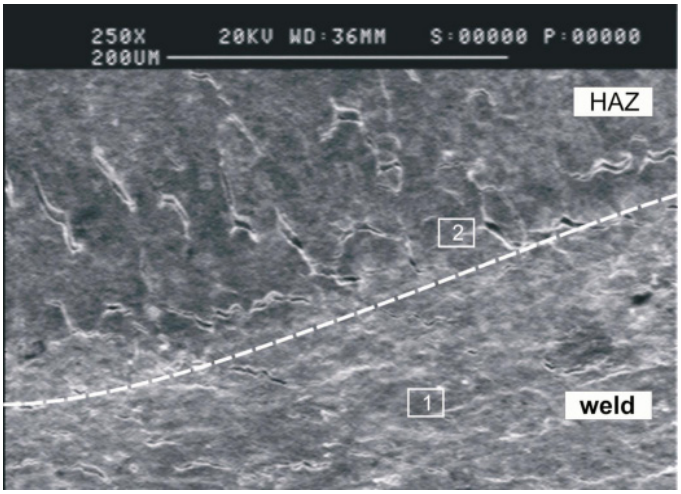

Fig. 11. SEM, surface cracks in the HAZ; places of the EDS microanalysis are marked as "1" and "2"

TABLE 3

The results of the surface microanalysis from Fig. 11

Place of analysis	Concentration of elements, wt %			
	Cr	Ni	Cu	O_2
Area 1 (joint)	18.75	7.91	5.49	8.12
Area 2 (HAZ next to the fusion line)	19.26	7.07	7.25	8.40
HAZ approx. 0.5 mm from the fusion line	19.97	7.25	6.36	8.71
The area of the base material	17.77	8.31	3.24	4.05

The average content of Cu is approx. 6.8% for the fusion line which is twice the average Cu content in the X10CrNiCuNb18-9-3 steel. EDS analysis of the HAZ areas located further in the direction of base material has shown that the copper content is approx. 5%, and thus exceeds the Cu content in the steel. Analysis of the chemical composition of the area outside the HAZ (approx. 3.3% Cu) showed no deviations from the mean value of Cu in the investigated steel.

4. Discussion

The investigations showed that X10CrNiCuNb18-9-3 austenitic stainless steel is very susceptibility to hot cracking.

Analysis of the microscopic observations that the X10CrNiCuNb18-9-3 austenitic steel with addition of Cu is more susceptible to solidification cracking than X5CrNi18-10 steel without addition of Cu. This is also confirmed by calculations based on R_{Cr}/R_{Ni}. The R_{Cr}/R_{Ni} calculated values for X10CrNiCuNb18-9-3 steel is 1.6, however for X5CrNi18-9-3 steel it is 1.62. The value of R_{Cr}/R_{Ni} ratio is $1{,}48 \leq R_{Cr}/R_{Ni} \leq 1{,}95$ therefore, according to the reference [11], both steels solidify with the separation of primary ferrite. However, the steel with the addition of Cu has a slightly lower R_{Cr}/R_{Ni} ratio, which indicates that there is more austenite in the microstructure of the weld. Therefore the X10CrNiCuNb18-9-3 steel has a higher tendency to solidification cracking. In addition, a large crack length a maximum of approx. 1.5 mm indicates a wide range of solidification temperatures of the X10CrNiCuNb18-9-3 steel, and therefore the high solidification cracking susceptibility of the studied steel.

The cause of high susceptibility to liquation cracking is associated with the niobium carbonitrides that are arranged in segregation bands (Fig. 8-9). On the basis of the studies a mechanism of cracking due to the equilibrium segregation during fusing the HAZ (Fig. 12) was proposed.

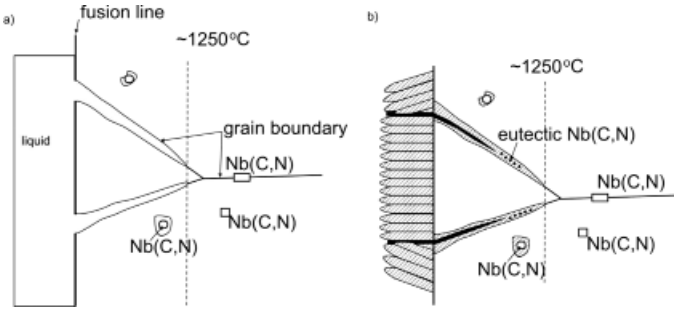

Fig. 12. The diagram showing the mechanism of cracking in the HAZ as a result of the equilibrium melting: a) fusion grain boundaries during the heating cycle, b) solidification and formation of the liquation cracks during the cooling cycle

The steel is melted during the heating cycle, and the migrating grain boundaries in the high-temperature region of the HAZ are anchored at the Nb (C, N) niobium carbonitrides. At the temperatures above approx. 1250°C a rapid dissolution of niobium carbonitrides occurs. As a result of this dissolution, some regions of austenite locally reach the eutectic composition and this is followed by the formation of liquid. The resulting liquid wets well the grain boundaries and under the stress this melt fills the regions at the grain boundaries.

During the cooling, liquid is quickly cooled below the temperature of the eutectic (g+ Nb(C,N)). The solidification of the eutectic melt and the shrinkage caused by this results in appearance of the cracks on the grain boundaries. Examples of the presented cracking mechanism are illustrated in Fig. 7-8. The carbides located inside the grains are also melted (Fig. 9).

Analysis of the surface cracks in X10CrNiCuNb18-9-3 steel showed that this steel is also very susceptible to surface cracks or superficial damage of the grain boundaries (Fig. 10). The data presented in Table 3 shows that the surface of the high-temperature HAZ area contains more than two times more Cu than it the average content of Cu in the steel. Furthermore, a slight increase in the chromium content, oxygen content and decrease of the nickel concentration were observed. These changes in chemical composition should be associated with the process of evaporation of components from the welding puddle and their oxidation as well as the re-deposition of the elements on the surface of the HAZ. A similar tendency to cracking was observed in the HAZ of the other precipitation hardened stainless steels with Cu [12]. These cracks are intergranular, and the oxidized inner surface suggests that the hot cracking occurs. The reason of the HAZ enriched in copper is intense evaporation of the welding paddle. Copper has the lowest evaporation temperature (2562°C) compared to nickel (2913°C) and chromium, which is (2672°C). If the welding is carried out using shielding gas (e.g. argon), the vapors of Cu are deposited in the HAZ. In spite of the shielding gas, oxidation of Cu vapors is also possible due vicinity of the air and the subsequent deposition of coper oxides. The copper oxides have a melting temperature of about 1200°C and the temperature of the Cu_2O-Cu eutectic is 1065°C. Thus, at the surface of the steel, a liquid layer of Cu or copper oxide could be present, in the region adjacent the weld, which is heated to a temperature of about 1100°C. The presence of a thin liquid layer and tensile stress during the test Transvarestraint causes intergranular fracture called Liquid Metal Embrittlement (LME) [13-16]. The cracks spread to a depth of 20-30 microns. This is the depth at which the small amount liquid is able to.

5. Summary

The present study showed that X10CrNiCuNb18-9-3 austenitic stainless steel is more susceptible to solidification cracking compared to X5CrNi18-10 steel. The reason for high susceptibility to liquation cracking is the presence of niobium carbonitrides which are arranged in segregation bands. During welding, in the presence of the stress, equilibrium fusing of Nb(C,N) occurs. Solidification of the eutectic and the shrinkage associated shrinkage with this causes the appearance of cracks on the grain boundaries. In this steel the presence of surface cracks which are integranular, it is also possible. The area where the cracks are observed show also enrichment in copper. The presence of stress and the strain caused by them, together with the presence of areas enriched in copper, leads to LME cracking.

In spite the fact that of the occurrence of cracks during welding the X10CrNiCuNb18-9-3 steel is observed, it may be a better alternative than steel X5CrNi18-10, for the construction of tubes, and the elements of boilers operating at high temperatures. With the addition of 3% Cu, the creep strength was increased, and the material can be operated at higher temperatures. One should be careful when joining the individual welded elements, and then perform thorough penetration weld testing. The X10CrNiCuNb18-9-3 steel is also better because of the difficult working conditions of the material. The corrosion resistance in this case is higher, which significantly extends the life time of the boiler components [1,4].

Acknowledgements

The research was carried out within the statutory research project no 11.11.110.299

REFERENCES

[1] J. Dobrzański, A. Zieliński, H. Purzyńska, Prace IMŻ **3**, 13-28 (2014).
[2] J. Pasternak, J. Dobrzanski, Advanced Materials Research **278**, 466-471 (2011).
[3] M. Vinoth Kumar, V. Balasubramanian, Int. J. Pres. Ves. Pip. **113**, 25-31 (2014).
[4] A. Zieliński, Journal of Achievements in Materials and Manufacturing Engineering **57**(2), 68-75 (2013).
[5] I. Sen, E. Amankwah, N.S. Kumar, E. Fleury, K. Oh-ishi, K. Hono, U. Ramamurty, Mat. Sci. Eng. A **528**, (13-14), 4491-4499 (2011).
[6] A. Ziewiec, E. Tasak, Metallurgical problems of welding of Super 304H steel, II Conference of Welding Powerwelding 2011, Kroczyce, Ostaniec 8-9 september 2011, 189-196 (2011).
[7] http://www.smsttubes.com.
[8] A. Zieliński, Journal of Achievements in Materials and Manufacturing Engineering **55**(2), 403-409 (2012).
[9] E. Tasak, A. Ziewiec, Wedability of Structural Materials. Tom1. Wedability of Steel, in Polish, Jak, Kraków (2009).
[10] J.N. DuPont, J.C. Lippold, S.D. Kiser, Welding Metallurgy and Weldability of Nickel-Base Alloys Wiley & Sons, Inc., Hoboken, New Jersey (2009).
[11] E. Tasak, Metallurgy of Welding, in Polish, Jak, Kraków, 2008.
[12] A. Ziewiec, E. Tasak, J. Czech, Arch. Metall. Mater. **50** (3), 1055-1061 (2012).
[13] H. Inoue, R. Matsuhashi, Y. Tadokoro, S. Fukumoto, T. Hashimoto, M. Mizumoto, H. Nagasaki, Nippon Steel Technical Report **95**, 22-27, January (2007).
[14] S. Rao, A.Y. Al-Kawaie, Weld. J. **89**(2), 46-49 (2010).
[15] L.G. Garza, C.J. Van Tyne, J. Mater. Process. Technol. **159**, 169-180 (2005).
[16] K. Pańcikiewicz, L. Tuz, A. Zielińska-Lipiec, Eng Failure Analysis **39**, 149-154 (2014).